Electronic Supplementary Material (ESI) for Journal of Materials Chemistry A.
This journal is © The Royal Society of Chemistry 2019

Electronic Supplementary Information (ESI) for

Ultrafast Li-Ion Migration in Holey-Graphene-Based Composites Constructed by A Generalized *Ex-Situ* Method towards High Capacity Energy Storage

Chengling Zhu,[a1] Zeyu Hui,[a1] Hui Pan,[a] Shenmin Zhu,*[a] Qing Zhang,[b] Jianfeng Mao,*[b] Zaiping Guo,*[bc] Yao Li,[a] Muhammad Imtiaz[ad] and Zhixin Chen[c]

[a]State Key Laboratory of Metal Matrix Composites, Shanghai Jiao Tong University, Shanghai 200240, China. E-mail: smzhu@sjtu.edu.cn

[b]Institute for Superconducting & Electronic Materials, Australian Institute of Innovative Materials, University of Wollongong, Wollongong 2522, Australia. E-mail: jmao@uow.edu.au; zguo@uow.edu.au

[c]Engineering Materials Institute, School of Mechanical, Materials & Mechatronics Engineering, University of Wollongong, Wollongong, 2522, Australia

[d]Department of Physics, Islamia College Peshawar, Peshawar 25120, Pakistan

[1]These authors contributed equally to this work.

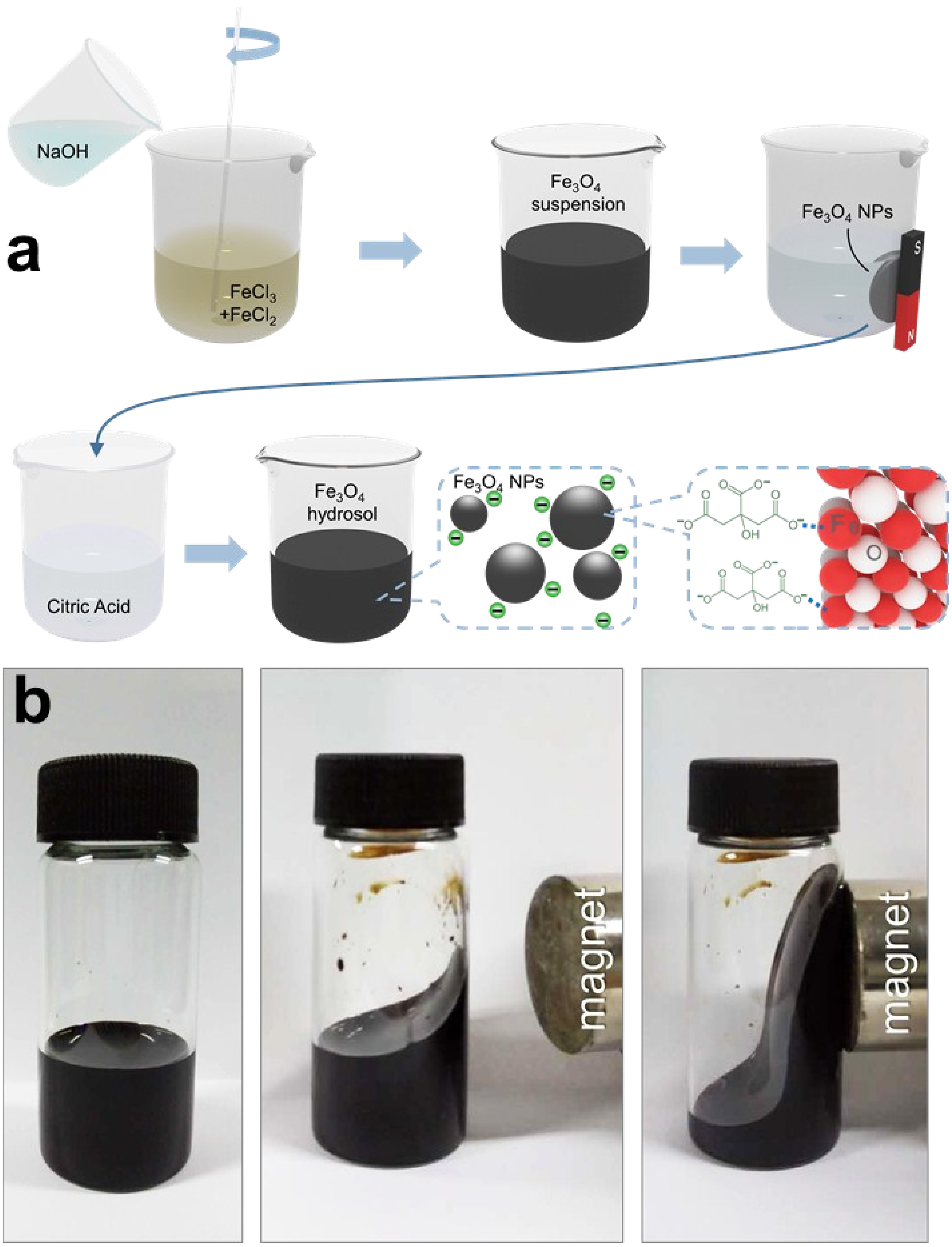

Fig. S1 (a) The schematic synthesis route of Fe_3O_4 hydrosol. (b) A simple demonstration to show the superparamagnetism of the Fe_3O_4 hydrosol, which is magnetofluid in fact.

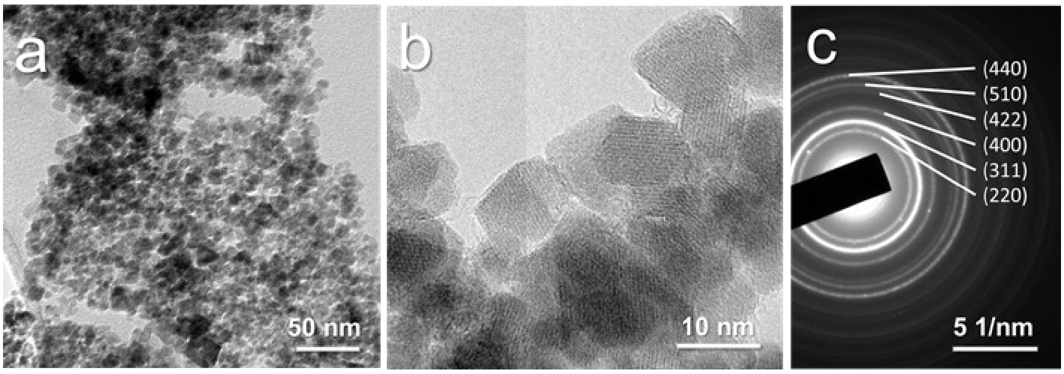

Fig. S2 TEM images and SAED pattern of the Fe_3O_4 nanoparticles.

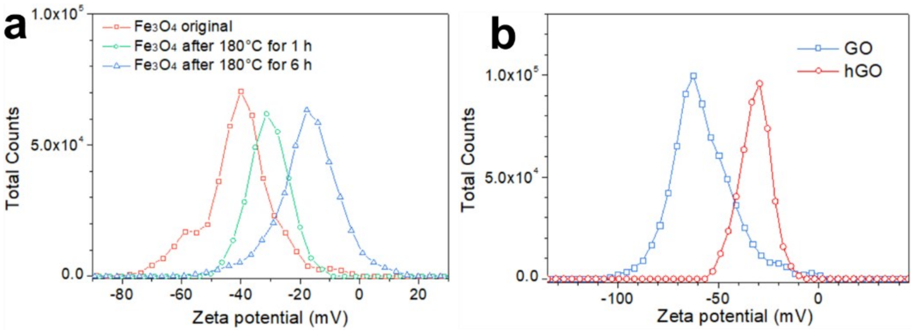

Fig. S3 (a) The zeta potential of Fe_3O_4 in the hydrosol, original and after hydrothermal process. This hydrothermal experiment was conducted on the Fe_3O_4 hydrosol solely to test its stability. (b) The zeta potential of GO and hGO.

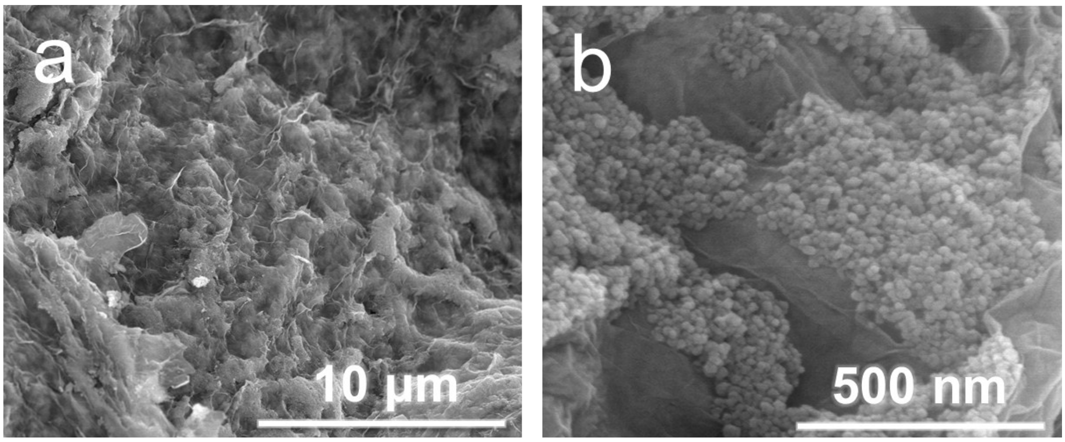

Fig. S4 SEM images of Fe_3O_4/G in (a) micron-scale and (b) submicron scale.

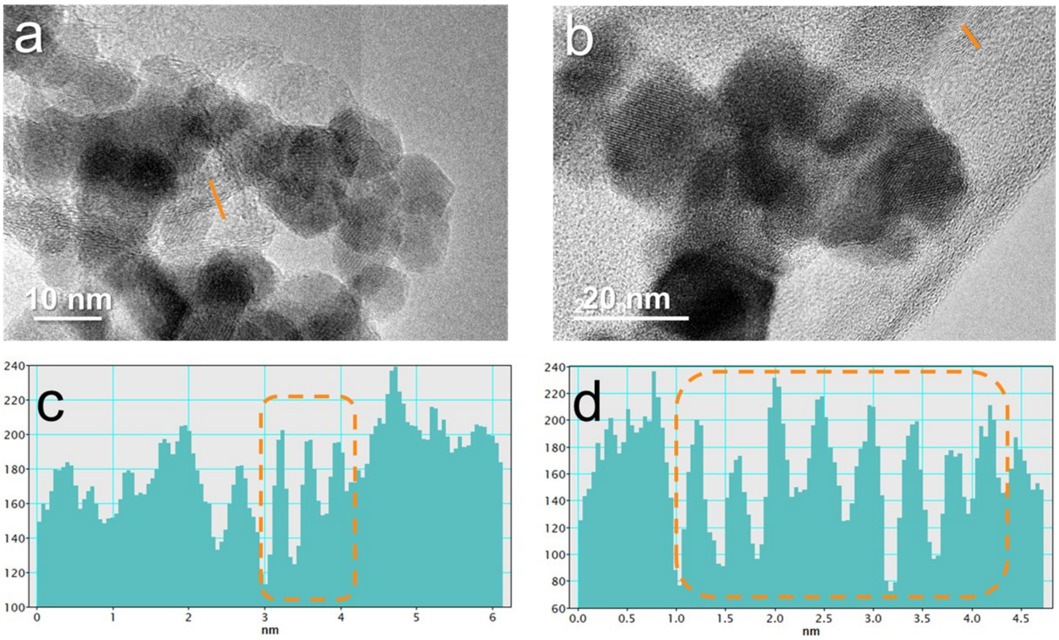

Fig. S5 TEM images of (a) Fe_3O_4@3DhG and (b) Fe_3O_4/G that rGO layers can be identified. (c, d) The line profiles of (a) and (b), respectively, with the orange boxes indicating rGO fringes.

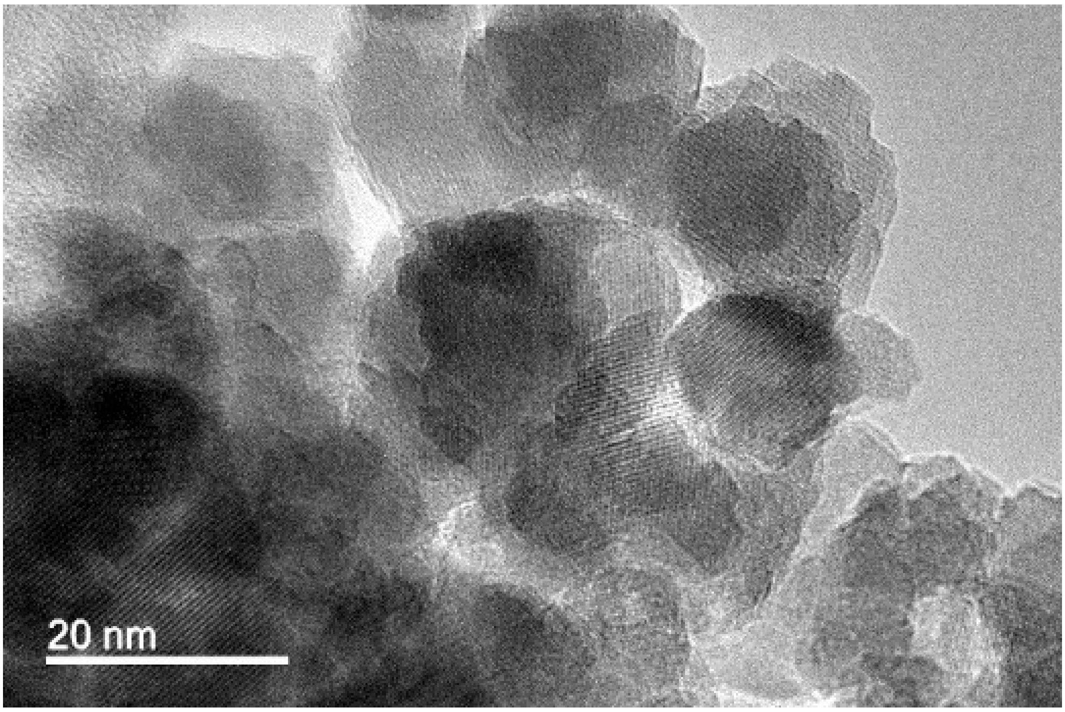

Fig. S6 HRTEM image of Fe_3O_4/G.

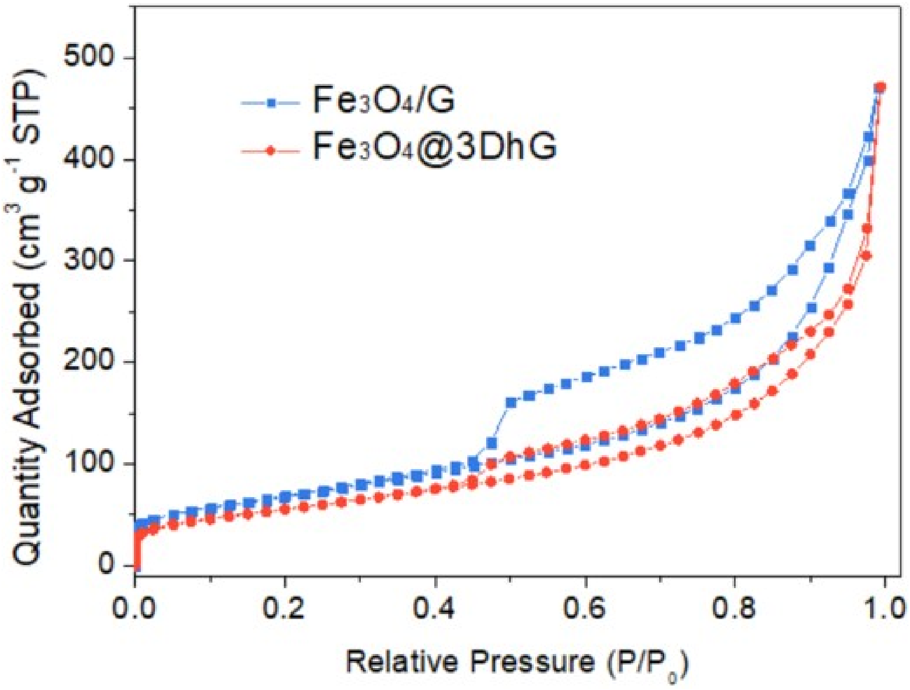

Fig. S7 The nitrogen adsorption isotherms of Fe_3O_4@3DhG and Fe_3O_4/G.

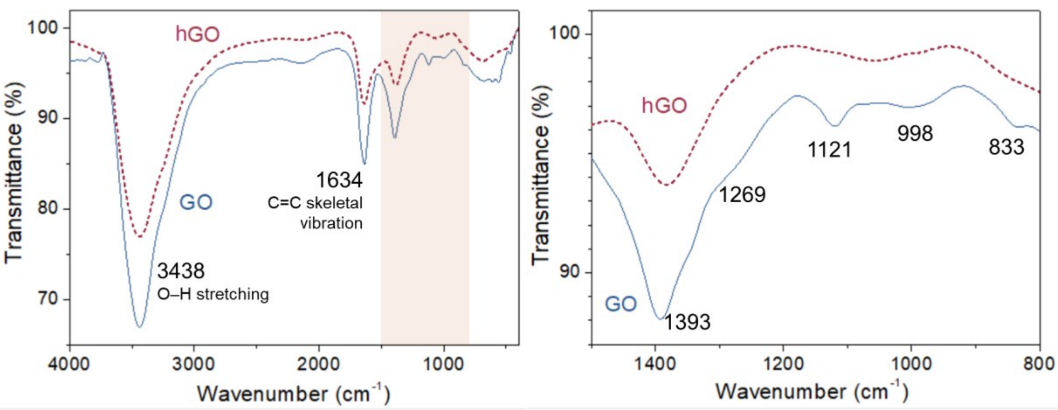

Fig. S8 (a) FT-IR spectra of hGO (red) and GO (blue). (b) The magnified part of (a) between 800-1500 cm^{-1}.

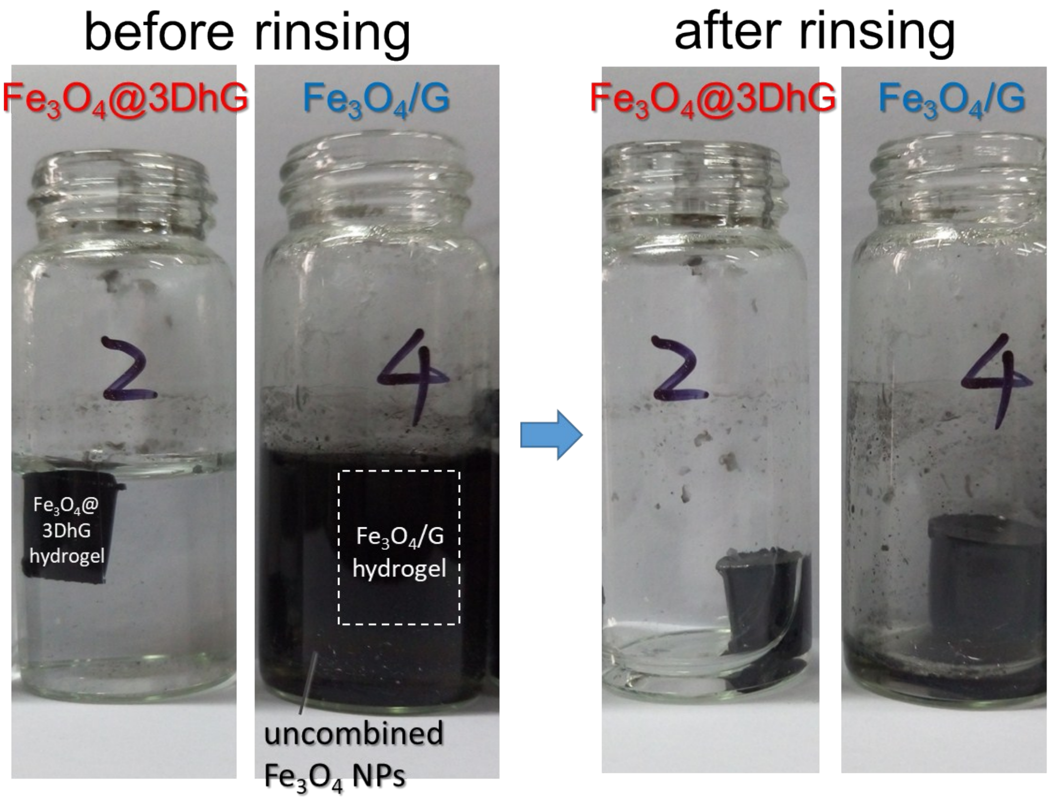

Fig. S9 Photos of Fe_3O_4@3DhG and Fe_3O_4/G after hydrothermal process. Many uncombined Fe_3O_4 NPs were found in the container of Fe_3O_4/G, and were removed after rinsing.

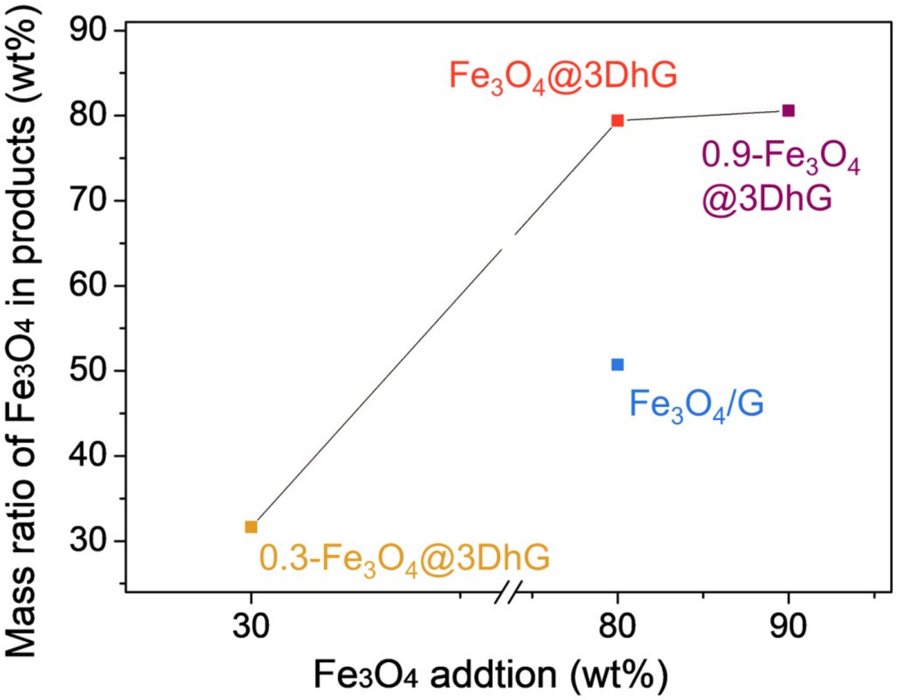

Fig. S10 The relation between the Fe_3O_4 addition and the mass ratio of Fe_3O_4 in products.

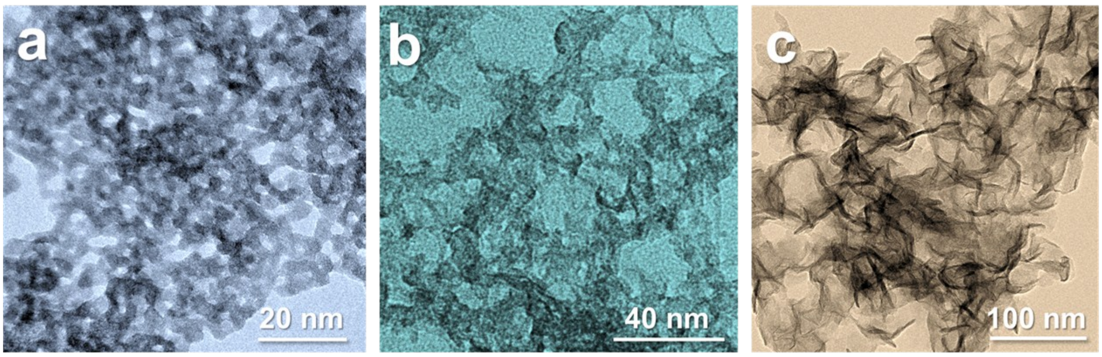

Fig. S11 TEM images of the (a) SnO_2 NPs, (b) δ-MnO_2 NPs and (c) MoS_2 NSs.

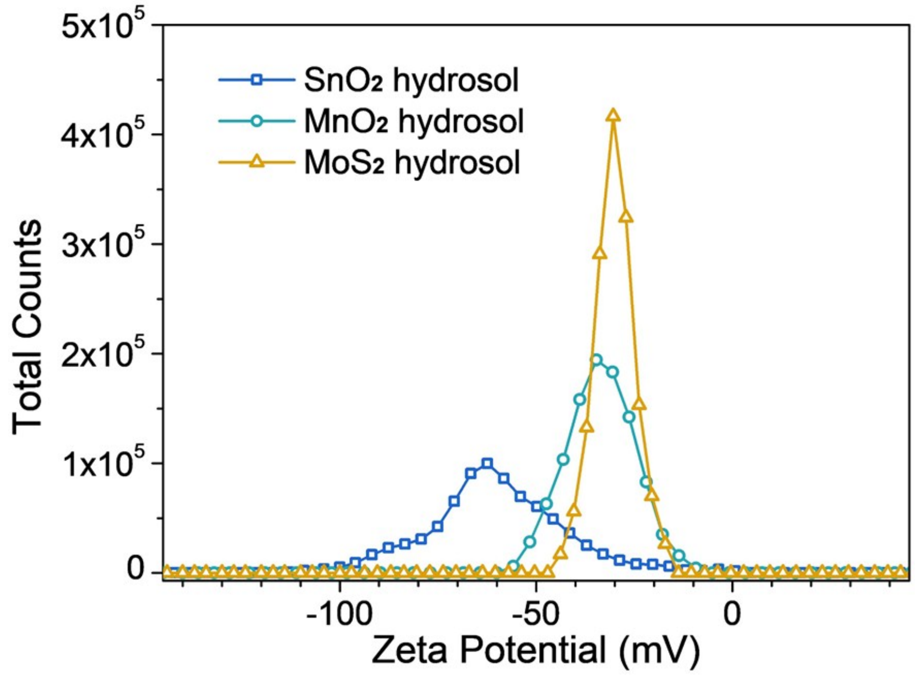

Fig. S12 The zeta potential of SnO_2 NPs, δ-MnO_2 NPs and MoS_2 NSs in corresponding hydrosols.

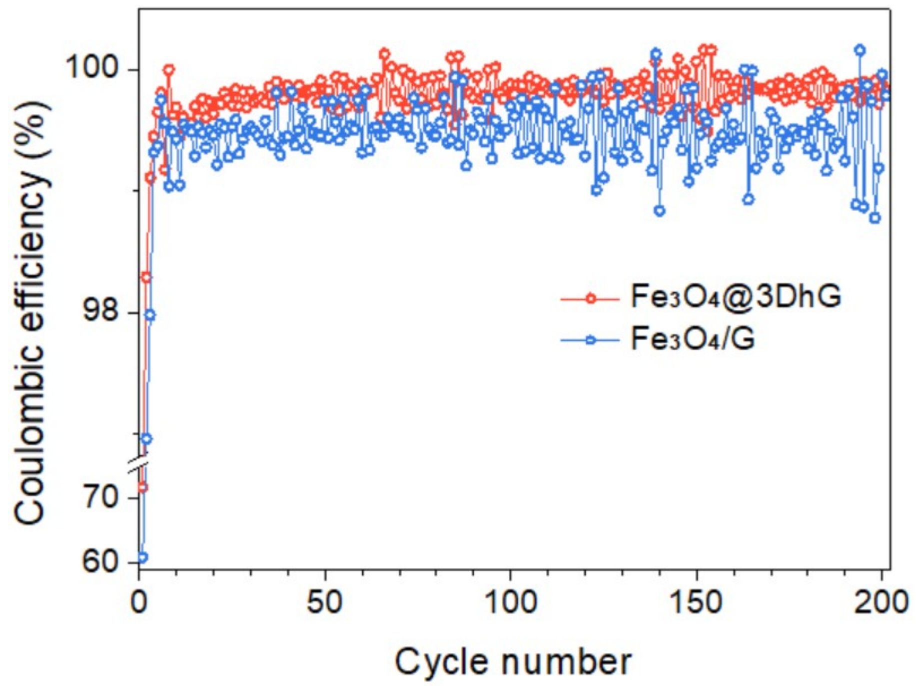

Fig. S13 The coulombic efficiency of Fe_3O_4@3DhG and Fe_3O_4/G half cells at 0.2 A g^{-1}.

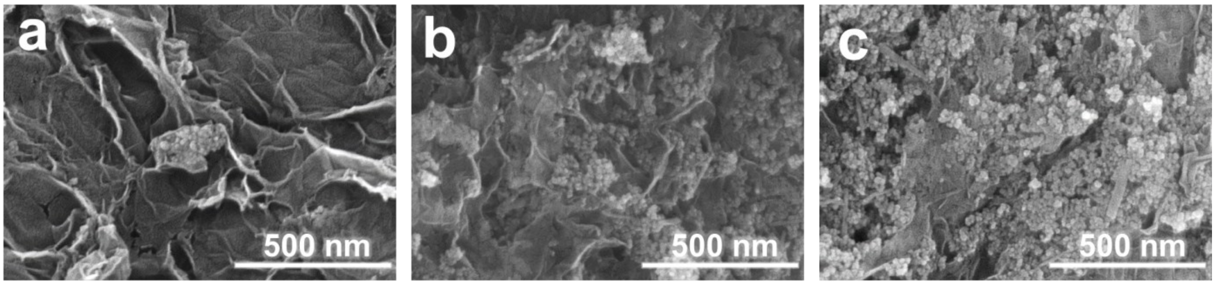

Fig. S14 SEM images of (a) 0.3-Fe_3O_4@3DhG, (b) Fe_3O_4@3DhG, and (c) 0.9-Fe_3O_4@3DhG.

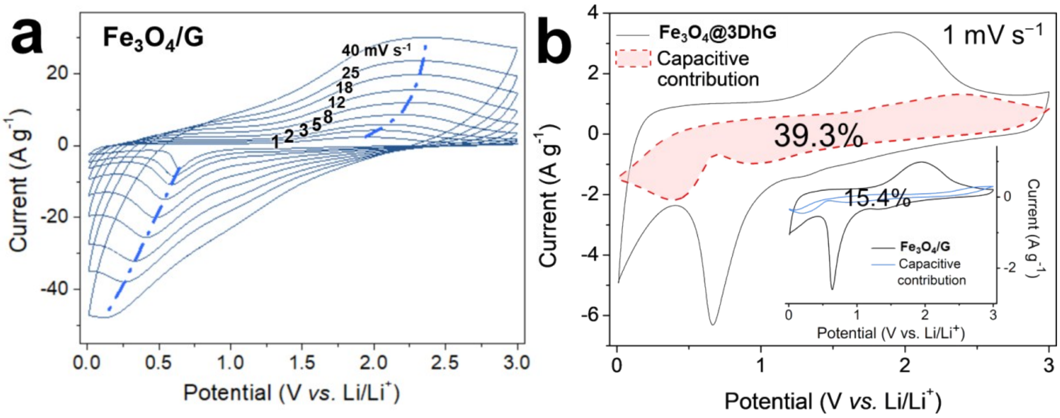

Fig. S15 (a) CV curves of Fe_3O_4/G at scan rates of 1−40 mV s^{-1}. (b) The calculated contribution of surface capacitive effect of Fe_3O_4@3DhG and (inset) Fe_3O_4/G at 1 mV s^{-1}.

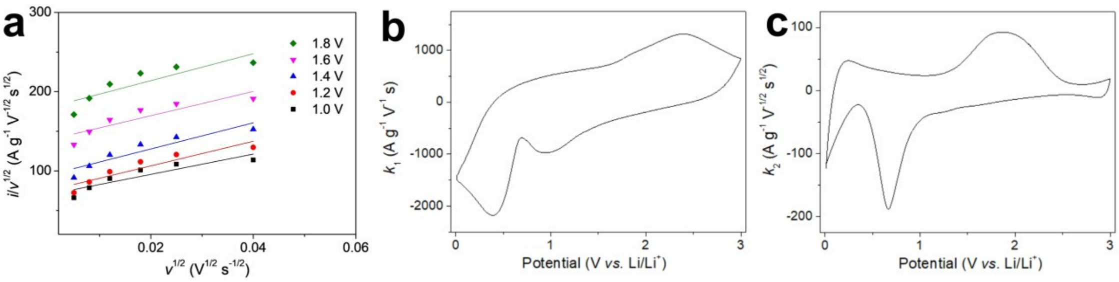

Fig. S16 (a) The example of linear fitting of $i/v^{1/2}$ *vs.* $v^{1/2}$ based on the data in Fig. 3a. The solved (b) k_1- and (c) k_2-value *vs.* potential.

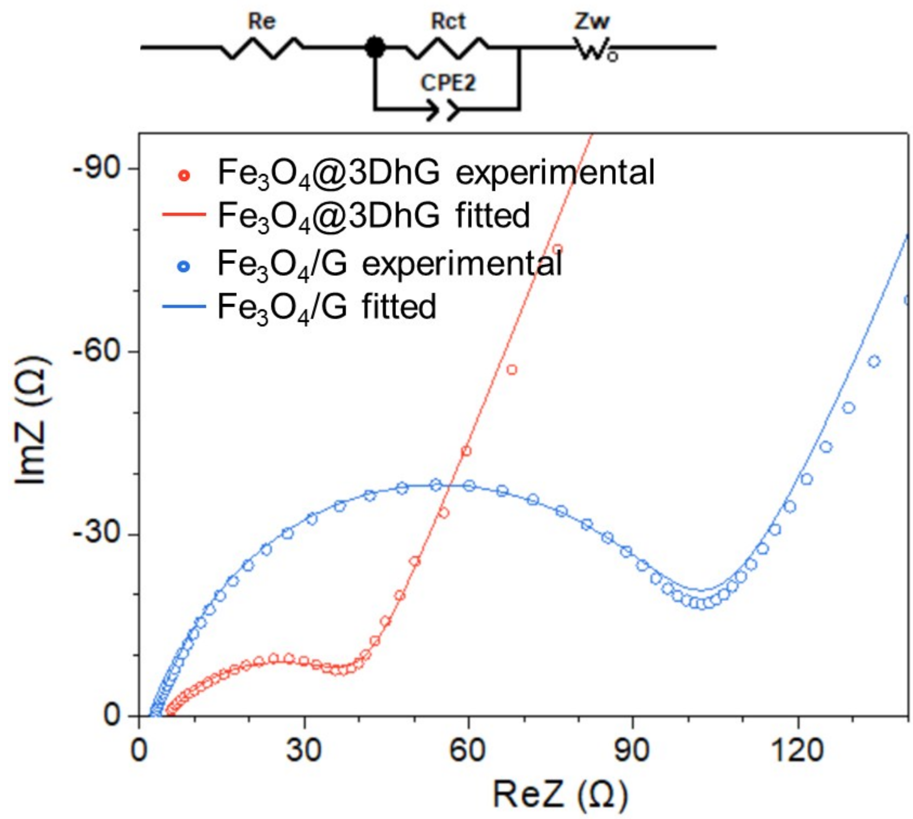

Fig. S17 The experimental and fitted Nyquist plots of Fe_3O_4@3DhG and Fe_3O_4/G before cycling test.

Table S1 The composition and performance of the reported **graphene-based** composites synthesized by *ex-situ*-combined method for LIB anodes.

Active Materials	Loading Content (wt%)	Particle Size (nm)	Capacity (mAh g^{-1})	Cycle Number	Current Density (A g^{-1})	Reference
SnO_2	48	5	924	200	0.1	1
			505	1000	1	
Si	32.8	<100	1261	70	0.05	2
MnO	84	100−200	1202	100	0.2	3
			812	1000	2	
Co_3O_4	76.2	270	600	500	1	4
Co_3S_4	70.8	30	710	200	0.5	5
ZnO	58	3.5	650	100	0.0978	6
Fe_2O_3	80	400	758	300	0.2	7
Fe_3O_4+TiO_2	60	6	703	200	0.5	8
Fe_3O_4	70.5	100	1048	50	0.2	9
			1080	450	1	
Fe_3O_4	83.7	200	1059	150	0.093	10
Fe_3O_4	63	57.6	550	60	0.375	11
Fe_3O_4	79.4	10	1516	200	0.2	**This Work**
			554	2000	5	

Table S2 The composition and performance of the reported iron oxide−graphene composites for LIB anodes in recent years.

Composition	Synthesis Route	Loading Content (wt%)	Particle Size (nm)	Capacity (mAh g^{-1})	Cycle Number	Current Density (A g^{-1})	Reference
Fe_3O_4@carbon microboxes	*ex situ*	/	650	857	100	0.1	12
Fe_3O_4 nanorods/rGO	*in situ*	75	10−80	1149	100	0.1	13
				1053	250	0.5	
Fe_3O_4-Fe@Bamboo-like CNT	*in situ*	34.4	70	764.1	100	0.3	14
Fe_3O_4/carbon/CNT microspheres	*in situ*	36.7	20	1317	130	0.1	15
				525	300	5	
Fe_3O_4/N-doped carbon	*in situ*	55	5	1963	170	0.1	16
				1741	600	1	
graphene@Fe_3O_4/amorphous carbon	*in situ*	37.4	2−3	853	500	0.2	17
Fe_3O_4/N-doped graphene	*in situ*	73.5	15	~1,200	150	0.1	18
				>900	1000	3	
Fe_3O_4/graphene foam	*in situ*	79.4	20−180	1220	500	1	19
hollow Fe_3O_4/carbon	*in situ*	67	100−120	1300	100	0.1	20
Fe_3O_4/C nanofibers	*ex situ*	27.7	30	780	150	0.5	21
				611	300	1	
Fe_3O_4 nanorods/N-doped graphene	*in situ*	85	20	929	50	0.1	22
Fe_3O_4/graphene	*in situ*	74.3	15	1070	160	0.2	23
				445	600	2	
Graphene-Wrapped Fe_3O_4 -Graphene Nanoribbons	*in situ*	60	10	708	300	0.4	24
Fe_3O_4@Polypyrrole Nanocages	*in situ*	88.7	650	652	500	2	25
				950	100	0.2	
Fe_3O_4/Graphene Nanoribbons	*in situ*	58	6	1700	100	0.1	26
				1058	100	1	
Fe_3O_4/Few layer Graphene	*ex situ*	73.4	10	1413	100	1	27
				768	100	5	
γ-Fe_2O_3/RGO	*in situ*	64	50	830	500	0.5	28
yolk−shell octahedron	*in situ*	/	400	1176	200	0.1	29
				744	500	1	
Fe_2O_3/C hollow microfibers	*in situ*	/	100	997.8	200	1	30
hollow Fe_2O_3/C Nanofibers	*in situ*	62	17	812	300	1	31
Porous Fe_2O_3 Nanoframeworks/Graphene	*in situ*	66.7	20−40	1129	130	0.2	32
				523.5	1200	5	
nitridated α-Fe_2O_3 nanorods/carbon cloth	*in situ*	/	100−300	332	100	5	33

Porous α-Fe_2O_3 nanorods/CNT/graphene	*in situ*	/	50	~1200	300	0.2	34
Fe_2O_3/few layered graphene	*ex situ*	~75	28	729	300	0.2	7
Monolithic Fe_2O_3/graphene hybrid	*in situ*	42	30-50	810	100	0.1	35
α-Fe_2O_3/GO/CNTs	*in situ*	83	50	875	100	0.2	36
α-Fe_2O_3/Graphene	*in situ*	48.3	180	1111.6	350	0.2	37
				658.5	200	1	
α-Fe_2O_3 Hollow Nanobarrels/rGO	*in situ*	52	200	916	100	0.5	38
				478	1000	5	
Hollow Fe_2O_3/N-Doped Graphene	*in situ*	86	30	1483	100	0.1	39
				729	300	1	
Fe_2O_3/Fe_3C−Graphene Thin Films	*in situ*	24	40	984	100	0.17	40
				518	1000	6.6	
FeOOH/rGO	*in situ*	81.4	200	1135	200	1	41
				783	200	5	
Fe_3O_4@3DhG	*ex situ*	79.4	10	1516	200	0.2	**This Work**
				554	2000	5	

Reference:

1 C. Zhu, S. Zhu, K. Zhang, Z. Hui, H. Pan, Z. Chen, Y. Li, D. Zhang and D.-W. Wang, *Sci. Rep.,* 2016, **6**, 25829.

2 H. Tang, Y. Zhang, Q. Xiong, J. Cheng, Q. Zhang, X. Wang, C. Gu and J. Tu, *Electrochim. Acta,* 2015, **156**, 86-93.

3 Y. Zhang, P. Chen, X. Gao, B. Wang, H. Liu, H. Wu, H. Liu and S. Dou, *Adv. Funct. Mater.,* 2016, **26**, 7754-7765.

4 H. Sun, X. Sun, T. Hu, M. Yu, F. Lu and J. Lian, *J. Phys. Chem. C,* 2014, **118**, 2263-2272.

5 Y. Du, X. Zhu, X. Zhou, L. Hu, Z. Dai and J. Bao, *J. Mater. Chem. A,* 2015, **3**, 6787-6791.

6 R. Guo, W. Yue, Y. An, Y. Ren and X. Yan, *Electrochim. Acta,* 2014, **135**, 161-167.

7 Y. Wang, L. Yang, R. Hu, W. Sun, J. Liu, L. Ouyang, B. Yuan, H. Wang and M. Zhu, *J. Power Sources,* 2015, **288**, 314-319.

8 L. Pan, X. D. Zhu, X. M. Xie and Y. T. Liu, *Adv. Funct. Mater.,* 2015, **25**, 3341-3350.

9 Y. Yang, J. Li, D. Chen and J. Zhao, *ACS Appl. Mater. Interfaces,* 2016, **8**, 26730-26739.

10 W. Wei, S. Yang, H. Zhou, I. Lieberwirth, X. Feng and K. Müllen, *Adv. Mater.,* 2013, **25**, 2909-2914.

11 S. Petnikota, H. Maseed, V. Srikanth, M. Reddy, S. Adams, M. Srinivasan and B. Chowdari, *J. Phys. Chem. C,* 2017, **121**, 3778-3789.

12 H. Tian, H. Liu, T. Yang, J.-P. Veder, G. Wang, M. Hu, S. Wang, M. Jaroniec and J. Liu, *Mater. Chem. Front.,* 2017, **1**, 823-830.

13 W. Huang, X. Xiao, C. Engelbrekt, M. Zhang, S. Li, J. Ulstrup, L. Ci, J. Feng, P. Si and Q. Chi, *Mater. Chem. Front.,* 2017, **1**, 1185-1193.

14 L. Du, C. Xu, J. Liu, Y. Lan and P. Chen, *Nanoscale,* 2017, **9**, 14376-14384.

15 W. Han, X. Qin, J. Wu, Q. Li, M. Liu, Y. Xia, H. Du, B. Li and F. Kang, *Nano Research,* 2018, **11**, 892-904.

16 Y. Wang, Y. Gao, J. Shao, R. Holze, Z. Chen, Y. Yun, Q. Qu and H. Zheng, *Journal of Materials Chemistry A,* 2018.

17 C. Li, Z. Li, X. Ye, X. Yang, G. Zhang and Z. Li, *Chem. Eng. J.,* 2018, **334**, 1614-1620.

18 W. Qi, X. Li, H. Li, W. Wu, P. Li, Y. Wu, C. Kuang, S. Zhou and X. Li, *Nano Research,* 2017, **10**, 2923-2933.

19 Y. Huang, Z. Xu, J. Mai, T.-K. Lau, X. Lu, Y.-J. Hsu, Y. Chen, A. C. Lee, Y. Hou and Y. S. Meng, *Nano Energy,* 2017, **41**, 426-433.

20 Z. Yang, D. Su, J. Yang and J. Wang, *J. Power Sources,* 2017, **363**, 161-167.

21 Q. Wu, R. Zhao, X. Zhang, W. Li, R. Xu, G. Diao and M. Chen, *J. Power Sources,* 2017, **359**, 7-16.

22 J. Jiao, W. Qiu, J. Tang, L. Chen and L. Jing, *Nano Research,* 2016, **9**, 1256-1266.

23 Y. Dong, K. C. Yung, R. Ma, X. Yang, Y.-S. Chui, J.-M. Lee and J. A. Zapien, *Carbon,* 2015, **86**, 310-317.

24 L. Li, A. Kovalchuk, H. Fei, Z. Peng, Y. Li, N. D. Kim, C. Xiang, Y. Yang, G. Ruan and J. M. Tour, *Adv. Energy Mater.,* 2015, **5**.

25 J. Liu, X. Xu, R. Hu, L. Yang and M. Zhu, *Advanced Energy Materials,* 2016, **6**.

26 X. Zhao, X. Li, S. Zhang, J. Long, Y. Huang, R. Wang and J. Sha, *J. Mater. Chem. A,* 2017, **5**, 23592-23599.

27 M. Huang, C. Chen, S. Wu and X. Tian, *J. Mater. Chem. A,* 2017, **5**, 23035-23042.

28 B. Xu, X. Guan, L. Y. Zhang, X. Liu, Z. Jiao, X. Liu, X. Hu and X. Zhao, *J. Mater. Chem. A,* 2018, **6**, 4048-4054.

29 W. Guo, W. Sun, L.-P. Lv, S. Kong and Y. Wang, *ACS Nano,* 2017, **11**, 4198-4205.

30 J. Sun, C. Lv, F. Lv, S. Chen, D. Li, Z. Guo, W. Han, D. Yang and S. Guo, *ACS Nano,* 2017, **11**, 6186-6193.

31 J. S. Cho, Y. J. Hong and Y. C. Kang, *ACS Nano,* 2015, **9**, 4026-4035.

32 T. Jiang, F. Bu, X. Feng, I. Shakir, G. Hao and Y. Xu, *ACS Nano,* 2017, **11**, 5140-5147.

33 M.-S. Balogun, Z. Wu, Y. Luo, W. Qiu, X. Fan, B. Long, M. Huang, P. Liu and Y. Tong, *J. Power Sources,* 2016, **308**, 7-17.

34 M. Chen, J. Liu, D. Chao, J. Wang, J. Yin, J. Lin, H. J. Fan and Z. X. Shen, *Nano Energy,* 2014, **9**, 364-372.

35 L. Li, G. Zhou, Z. Weng, X.-Y. Shan, F. Li and H.-M. Cheng, *Carbon,* 2014, **67**, 500-507.

36 X. Ma, M. Zhang, C. Liang, Y. Li, J. Wu and R. Che, *ACS Appl. Mater. Interfaces,* 2015, **7**, 24191-24196.

37 X. Qi, H.-B. Zhang, J. Xu, X. Wu, D. Yang, J. Qu and Z.-Z. Yu, *ACS Appl. Mater. Interfaces,* 2017, **9**, 11025-11034.

38 K. S. Lee, S. Park, W. Lee and Y. S. Yoon, *ACS Appl. Mater. Interfaces,* 2016, **8**, 2027-2034.

39 L. Liu, X. Yang, C. Lv, A. Zhu, X. Zhu, S. Guo, C. Chen and D. Yang, *ACS Appl. Mater. Interfaces,* 2016, **8**, 7047-7053.

40 Y. Yang, X. Fan, G. Casillas, Z. Peng, G. Ruan, G. Wang, M. J. Yacaman and J. M. Tour, *ACS Nano,* 2014, **8**, 3939-3946.

41 H. Qi, L. Cao, J. Li, J. Huang, Z. Xu, Y. Cheng, X. Kong and K. Yanagisawa, *ACS Appl. Mater. Interfaces,* 2016, **8**, 35253-35263.